

LIDAR REMOTE SENSING DATA COLLECTION: Diablo Canyon, CA

Prepared for:



Prepared by:

WSI Corvallis Office
517 SW 2nd St,
Suite 400
Corvallis, OR 97333



Updated May 3, 2013

LIDAR REMOTE SENSING DATA COLLECTION: DIABLO CANYON, CA

Table of Contents

1. Overview	1
2. Acquisition	2
2.1 Airborne Survey - Flight Plan	2
2.2 Airborne Survey - Instrumentation and Methods	3
2.3 Ground Survey - Instrumentation and Methods.....	3
2.3.1 Survey Control	3
2.3.2 RTK Surveying.....	4
3. LiDAR Data Processing	6
3.1 Applications and Work Flow Overview	6
3.2 Aircraft Kinematic GPS and IMU Data.....	6
3.3 Laser Point Processing	7
4. LiDAR Accuracy Assessment	8
4.1 Laser Noise and Relative Accuracy	8
4.2 Absolute Accuracy	9
5. Study Area Results	9
5.1 Data Summary	9
5.2 Data Density/Resolution.....	9
5.3 Relative Accuracy Calibration Results	13
5.4 Absolute Accuracy	14
6. Orthophotos	16
7. WSI Deliverables	17
8. Selected Images	18
9. Glossary	21
10. Citations	21
Appendix A	22

1. Overview

Watershed Sciences, Inc. (WSI) collected Light Detection and Ranging (LiDAR) data on both the inland and intertidal land within the Diablo Canyon study area, located in San Luis Obispo County, California. The LiDAR was collected on January 28, 2010. The total area of delivered LiDAR, including a 100 meter buffer, (Figure 1) is 10,634 acres (43.03 square kilometers). This survey was flown as part of the Diablo Canyon Power Plant (DCCP) Long-Term Seismic Program (LTSP).

Figure 1. Overview of Diablo Canyon study area.



2. Acquisition

2.1 Airborne Survey – Flight Plan

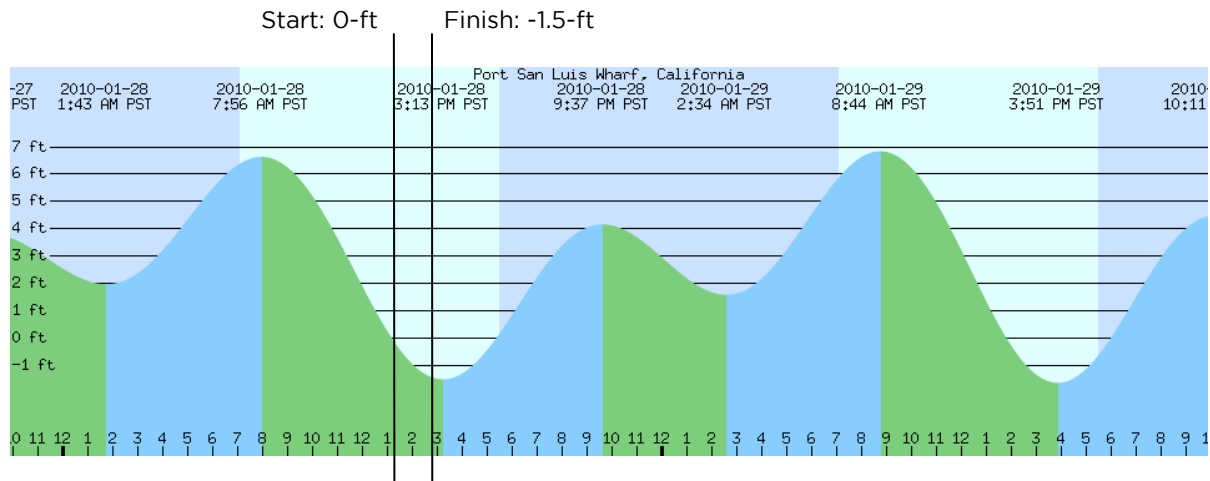
The LiDAR mission was planned to optimize coverage of areas exposed during the requested low tide windows (between 0.0 ft and peak low of ~-1.5 ft) and in conjunction with a PDOP value of less than 3.0. According to the Port San Luis Wharf Tidal Station database, a low tide window meeting these requirements occurred on January 28 and 29, between 1-4 PM, 2010.

The LiDAR acquisition required one full day of flying broken into two missions to capture the inland area as well as the tidal zone portion of the study area at a peak low tide. The first flight mission covered the inland portions of the study area while working toward the coastline. The second flight mission covered the tidal zone portion of the study area and occurred later in the day during the peak low tide (see Table 1 and Figure 2).

Table 1. Flight times for acquiring the intertidal land during low tide.

Day	Start Time	End Time
January	1:15 PM	2:54 PM

Figure 2. Port San Luis Wharf Tidal charts (35.1700° N, 120.7516° W) for January 28 and 29, 2010 displaying flying windows for capturing peak low tide.



2.2 Airborne Survey – Instrumentation and Methods

The LiDAR survey uses a Leica ALS50 Phase II laser system. For the intertidal land, the sensor scan angle was 313° from nadir¹ with a pulse rate designed to yield an average native density (number of pulses emitted by the laser system) of greater than, or equal to, eight pulses per square meter over terrestrial surfaces. All study areas were surveyed with an opposing flight line side-lap of $\geq 50\%$ ($\geq 100\%$ overlap) to reduce laser shadowing and increase surface laser painting. The Leica ALS50 Phase II system allows up to four range measurements (returns) per pulse, and all discernible laser returns were processed for the output dataset. It is not uncommon for some types of surfaces (e.g., dense vegetation or water) to return fewer pulses than the laser originally emitted. These discrepancies between ‘native’ and ‘delivered’ density will vary depending on terrain, land cover, and the prevalence of water bodies.

To accurately solve for laser point position (geographic coordinates x, y, z), the positional coordinates of the airborne sensor and the attitude of the aircraft were recorded continuously throughout the LiDAR data collection mission. Aircraft position was measured twice per second (two hertz) by an onboard differential GPS unit. Aircraft attitude was measured 200 times per second (200 hertz) as pitch, roll, and yaw (heading) from an onboard inertial measurement unit (IMU). To allow for post-processing correction and calibration, aircraft/sensor position and attitude data are indexed by GPS time.

2.3 Ground Survey – Instrumentation and Methods

The following ground survey data were collected to enable the geo-spatial correction of the aircraft positional coordinate data collected throughout the flight, and to allow for quality assurance checks on final LiDAR data products.

2.3.1 Survey Control

Simultaneous with the airborne data collection mission, multiple static (one hertz recording frequency) ground surveys were conducted over monuments with known coordinates (Table 2). Indexed by time, these GPS data are used to correct the continuous onboard measurements of aircraft position recorded throughout the mission. Multiple sessions were processed over the same monument to confirm antenna height measurements and reported position accuracy. After the airborne survey, these static GPS data were then processed using triangulation with Continuously Operating Reference Stations (CORS) stations, and checked against the Online Positioning User Service (OPUS²) to quantify daily variance. Controls were located within 13 nautical miles of the mission area.

¹ Nadir refers to the perpendicular vector to the ground directly below the aircraft. Nadir is commonly used to measure the angle from the vector and is referred to a “degrees from nadir”.

² Online Positioning User Service (OPUS) is run by the National Geodetic Survey to process corrected monument positions.

Table 2. Base Station Survey Control Coordinates for Diablo Canyon.

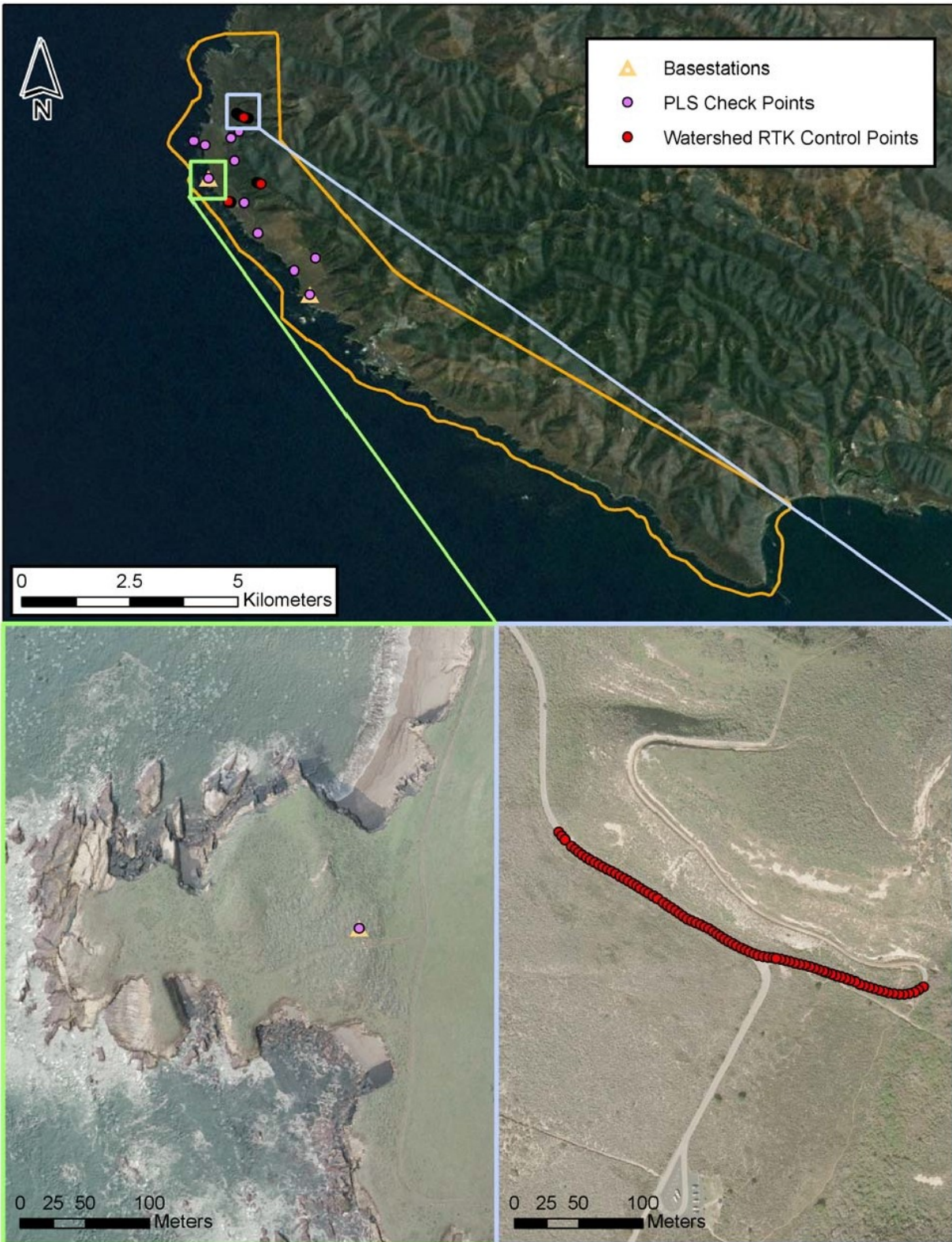
Base Station ID	Datum: NAD83 (CORS96)		
	Latitude	Longitude	Ellipsoid Z (meters)
Crowbar	35 13 20.82114	-120 52 12.90439	27.547
Vista02	35 14 49.88164	-120 53 44.39005	-15.034

2.3.2 RTK Surveying

To enable assessment of LiDAR data accuracy, ground truth points were collected using GPS based real-time kinematic (RTK) surveying. For an RTK survey, the ground crew uses a roving unit to receive radio-relayed corrected positional coordinates for all ground points from a GPS base station set up over a survey control monument. Instrumentation includes multiple Trimble DGPS units. RTK surveying allows for precise location measurements with an error (σ) of ≤ 2 cm (0.8 in). Figure 2 below portrays the distribution of all RTK point locations for the study area.



Figure 3. Watershed RTK and PLS control check point locations for the Diablo Canyon study area (129 RTK points collected by WSI).



3. LiDAR Data Processing

3.1 Applications and Work Flow Overview

1. Resolved kinematic corrections for aircraft position data using kinematic aircraft GPS and static ground GPS data.
Software: Waypoint GPS v.8.10, Trimble Geomatics Office v.1.62
2. Developed a smoothed best estimate of trajectory (SBET) file that blends post-processed aircraft position with attitude data. Sensor head position and attitude were calculated throughout the survey. The SBET data were used extensively for laser point processing.
Software: IPAS v.1.35
3. Calculated laser point position by associating SBET position to each laser point return time, scan angle, intensity, etc. Created raw laser point cloud data for the entire survey in *.las (ASPRS v. 1.2) format.
Software: ALS Post Processing Software v.2.7
4. Imported raw laser points into manageable blocks (less than 500 MB) to perform manual relative accuracy calibration and filter for pits/birds. Ground points were then classified for individual flight lines (to be used for relative accuracy testing and calibration).
Software: TerraScan v.9.017
5. Using ground classified points per each flight line, the relative accuracy was tested. Automated line-to-line calibrations were then performed for system attitude parameters (pitch, roll, heading), mirror flex (scale) and GPS/IMU drift. Calibrations were performed on ground classified points from paired flight lines. Every flight line was used for relative accuracy calibration.
Software: TerraMatch v.9.004
6. Position and attitude data were imported. Resulting data were classified as ground and non-ground points. Statistical absolute accuracy was assessed via direct comparisons of ground classified points to ground RTK survey data. Data were then converted to orthometric elevations (NAVD88) by applying a Geoid03 correction. Ground models were created as a triangulated surface and exported as ArcInfo ASCII grids at a three-foot pixel resolution.
Software: TerraScan v.9.017, ArcMap v. 9.3.1, TerraModeler v.9.003

3.2 Aircraft Kinematic GPS and IMU Data

LiDAR survey datasets were referenced to the one hertz static ground GPS data collected over pre-surveyed monuments with known coordinates. While surveying, the aircraft collected two hertz kinematic GPS data, and the onboard inertial measurement unit (IMU) collected 200 hertz aircraft attitude data. Waypoint Grafnav was used to process the kinematic corrections for the aircraft. The static and kinematic GPS data were then post-processed after the survey to obtain an accurate GPS solution and aircraft positions. Leica's IPAS Pro was used to develop a trajectory file that includes corrected aircraft position and attitude information. The trajectory data for the entire flight survey session were incorporated into a final smoothed best estimated trajectory (SBET) file that contains accurate and continuous aircraft positions and attitudes.

3.3 Laser Point Processing

Laser point coordinates were computed using the IPAS Pro software based on independent data from the LiDAR system (pulse time, scan angle), and aircraft trajectory data (SBET). Laser point returns (first through fourth) were assigned an associated (x, y, z) coordinate along with unique intensity values (0-255). The data were output into large LAS v. 1.1 files; each point maintains the corresponding scan angle, return number (echo), intensity, and x, y, z (easting, northing, and elevation) information.

These initial laser point files were too large for subsequent processing. To facilitate laser point processing, bins (polygons) were created to divide the dataset into manageable sizes (< 500 MB). Flightlines and LiDAR data were then reviewed to ensure complete coverage of the study area and positional accuracy of the laser points.

Laser point data were imported into processing bins in TerraScan, and manual calibration was performed to assess the system offsets for pitch, roll, heading and scale (mirror flex). Using a geometric relationship developed by WSI, each of these offsets was resolved and corrected if necessary.

LiDAR points were then filtered for noise, pits (artificial low points) and birds (true birds as well as erroneously high points) by screening for absolute elevation limits, isolated points and height above ground. Each bin was then manually inspected for remaining pits and birds and spurious points were removed. In a bin containing approximately 7.5-9.0 million points, an average of 50-100 points are typically found to be artificially low or high. Common sources of non-terrestrial returns are clouds, birds, vapor, haze, decks, brush piles, etc.

Internal calibration was refined using TerraMatch. Points from overlapping lines were tested for internal consistency and final adjustments were made for system misalignments (e.g., pitch, roll, heading offsets and scale). Automated sensor attitude and scale corrections yielded three to five centimeter improvements in the relative accuracy. Once system misalignments were corrected, vertical GPS drift was then resolved and removed per flight line, yielding a slight improvement (less than one centimeter) in relative accuracy.

The TerraScan software suite is designed specifically for classifying near-ground points (Soininen, 2004). The processing sequence began by 'removing' all points that were not 'near' the earth based on geometric constraints used to evaluate multi-return points. The resulting bare earth (ground) model was visually inspected and additional ground point modeling was performed in site-specific areas to improve ground detail. This manual editing of grounds often occurs in areas with known ground modeling deficiencies, such as bedrock outcrops, cliffs, deeply incised stream banks, and dense vegetation. In some cases, automated ground point classification erroneously included known vegetation (e.g., understory, low/dense shrubs). These points were manually reclassified as non-grounds. Ground surface raster models were developed from triangulated irregular networks (TINs) of ground points.

4. LiDAR Accuracy Assessment

Our LiDAR quality assurance process uses the data from the RTK ground survey conducted in the study area. In this project, a total of **129 RTK** GPS measurements were collected on hard, bare earth surfaces (e.g. asphalt) distributed among multiple flight swaths. To assess absolute accuracy, we compared the location coordinates of these known RTK ground survey points to those calculated for the closest laser points.

4.1 Laser Noise and Relative Accuracy

Laser point absolute accuracy is largely a function of laser noise and relative accuracy. To minimize these contributions to absolute error, we first performed a number of noise filtering and calibration procedures prior to evaluating absolute accuracy.

Laser Noise

For any given target, laser noise is the breadth of the data cloud per laser return (e.g., last, first). Lower intensity surfaces (e.g., roads, rooftops, still/calm water) experience higher laser noise. The laser noise range for this study was approximately 0.02 meters.

Relative Accuracy

Relative accuracy refers to the internal consistency of the data set (i.e., the ability to place a laser point in the same location over multiple flight lines, GPS conditions, and aircraft attitudes). Affected by system attitude offsets, scale, and GPS/IMU drift, internal consistency is measured as the divergence between points from different flight lines within an overlapping area. Divergence is most apparent when flight lines are opposing. When the LiDAR system is well calibrated, the line-to-line divergence is low (<10 cm). See Appendix A for further information on sources of error and operational measures that can be taken to improve relative accuracy.

Relative Accuracy Calibration Methodology

1. Manual System Calibration: Calibration procedures for each mission require solving geometric relationships that relate measured swath-to-swath deviations to misalignments of system attitude parameters. Corrected scale, pitch, roll and heading offsets were calculated and applied to resolve misalignments. The raw divergence between lines was computed after the manual calibration was completed and reported for each study area.
2. Automated Attitude Calibration: All data were tested and calibrated using TerraMatch automated sampling routines. Ground points were classified for each individual flight line and used for line-to-line testing. System misalignment offsets (pitch, roll, and heading) and scale were solved for each individual mission and applied to respective mission datasets. The data from each mission were then blended when imported together to form the entire area of interest.

3. Automated Z Calibration: Ground points per line were utilized to calculate the vertical divergence between lines caused by vertical GPS drift. Automated Z calibration was the final step employed for relative accuracy calibration.

4.2 Absolute Accuracy

The vertical accuracy of the LiDAR data is described as the mean and standard deviation (sigma - σ) of divergence of LiDAR point coordinates from RTK ground survey point coordinates. To provide a sense of the model predictive power of the dataset, the root mean square error (RMSE) for vertical accuracy is also provided. These statistics assume the error distributions for x, y, and z are normally distributed, thus we also consider the skew and kurtosis of distributions when evaluating error statistics. Statements of statistical accuracy apply to fixed terrestrial surfaces only.

5. Study Area Results

Summary statistics for point resolution and accuracy (relative and absolute) of the LiDAR data collected in Diablo Canyon study areas are presented below in terms of central tendency, variation around the mean, and the spatial distribution of the data (for point resolution by bin).

5.1 Data Summary

Table 3. Resolution and Accuracy - Specifications and Achieved Values

	Targeted	Achieved
Resolution:	> 8 points/m ²	8.84 points/m ²
Vertical Accuracy (1 σ):	<15 cm	4.0 cm

5.2 Data Density/Resolution

The first return laser point density was above the targeted density (Table 3). However, some types of surfaces (e.g., dense vegetation, breaks in terrain, steep slopes, water) may return fewer pulses (delivered density) than the laser originally emitted (native density). The surveyed area consisted of three main land cover types; water, sand/mud, and dense vegetation along the coast. The large amount of water in the surveyed area reduced the number of laser returns, but the overall native density still exceeded specification. Ground classifications were derived from automated ground surface modeling and manual, supervised classifications where it was determined that the automated model had failed. Ground return densities will be lower in areas of dense vegetation, water, or buildings.

Data Resolution for the Diablo Canyon study area:

- Average Point (First Return) Density = 8.84 points/m²
- Average Ground Point Density = 2.34 points/m²

Figure 4. Density distribution for first return laser points

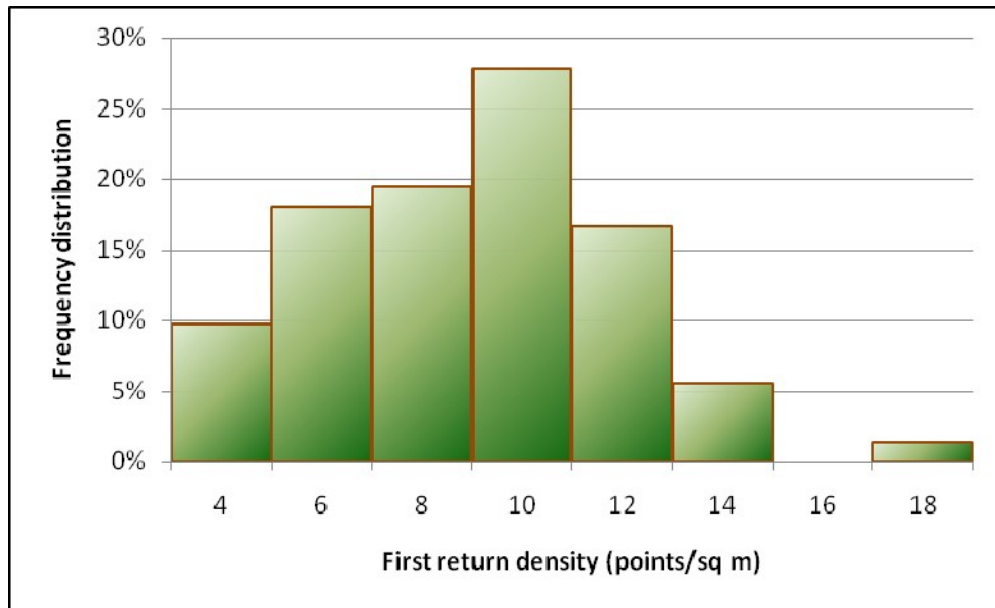


Figure 5. Density distribution for ground-classified laser points.

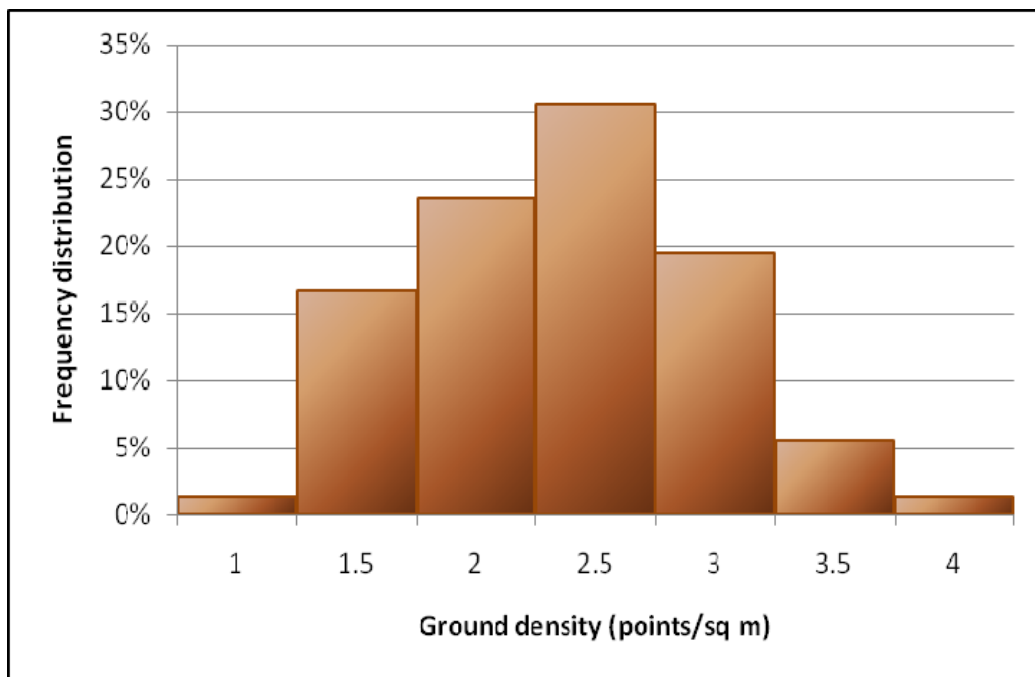


Figure 6. First return laser point data density per processing bin

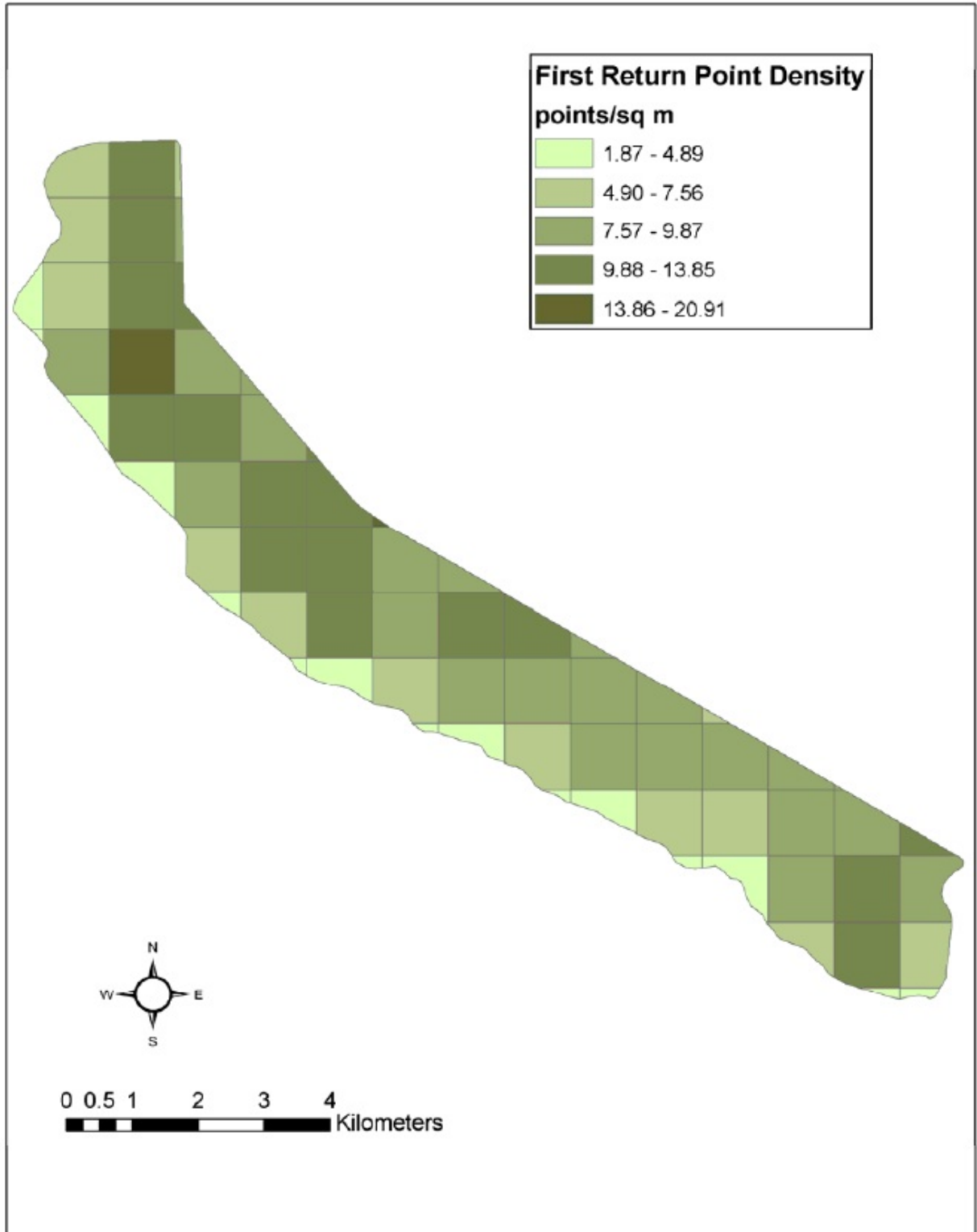
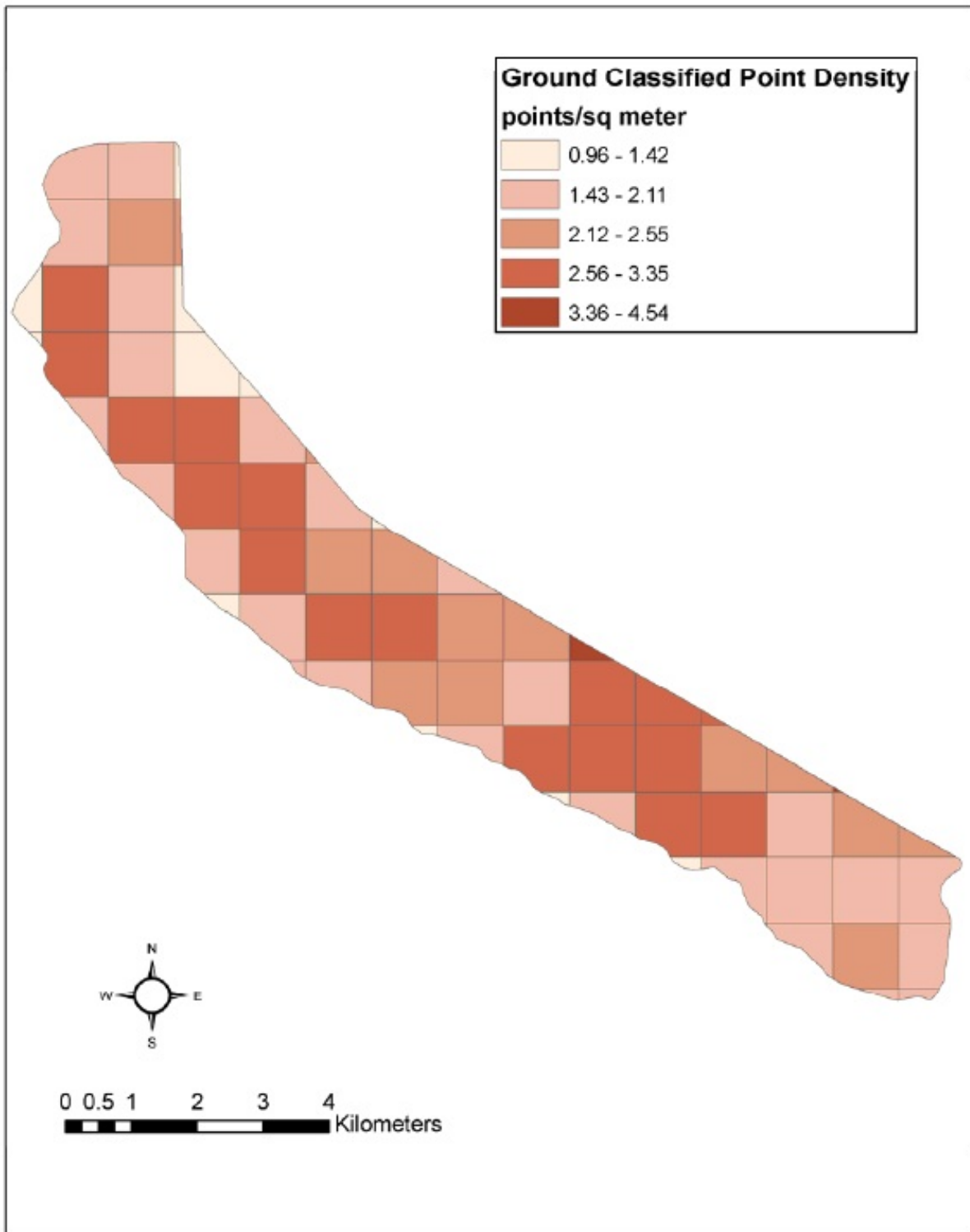


Figure 7. Ground-classified laser point data density per processing bin

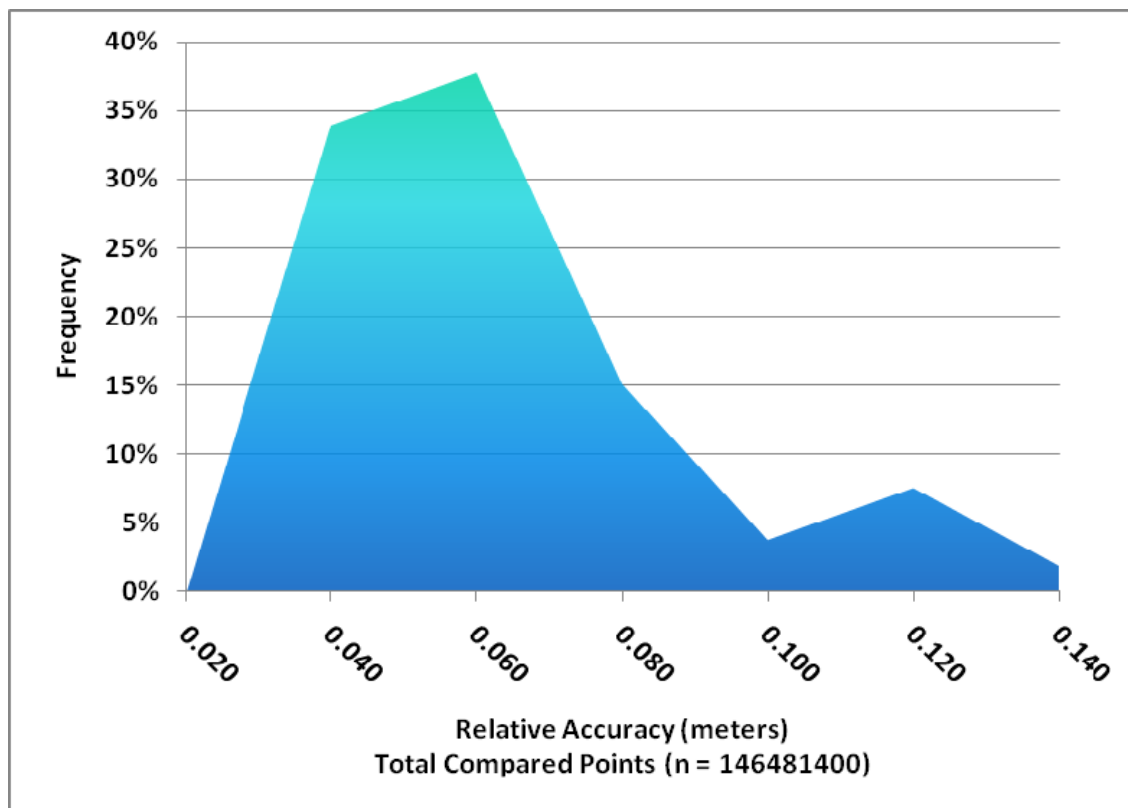


5.3 Relative Accuracy Calibration Results

Relative accuracies for the intertidal land within the Diablo Canyon study area:

- Project Average = 0.054 cm
- Median Relative Accuracy = 0.044 cm
- 1σ Relative Accuracy = 0.058 cm
- 2σ Relative Accuracy = 0.111 cm

Figure 8. Distribution of relative accuracies per flight line, non slope-adjusted



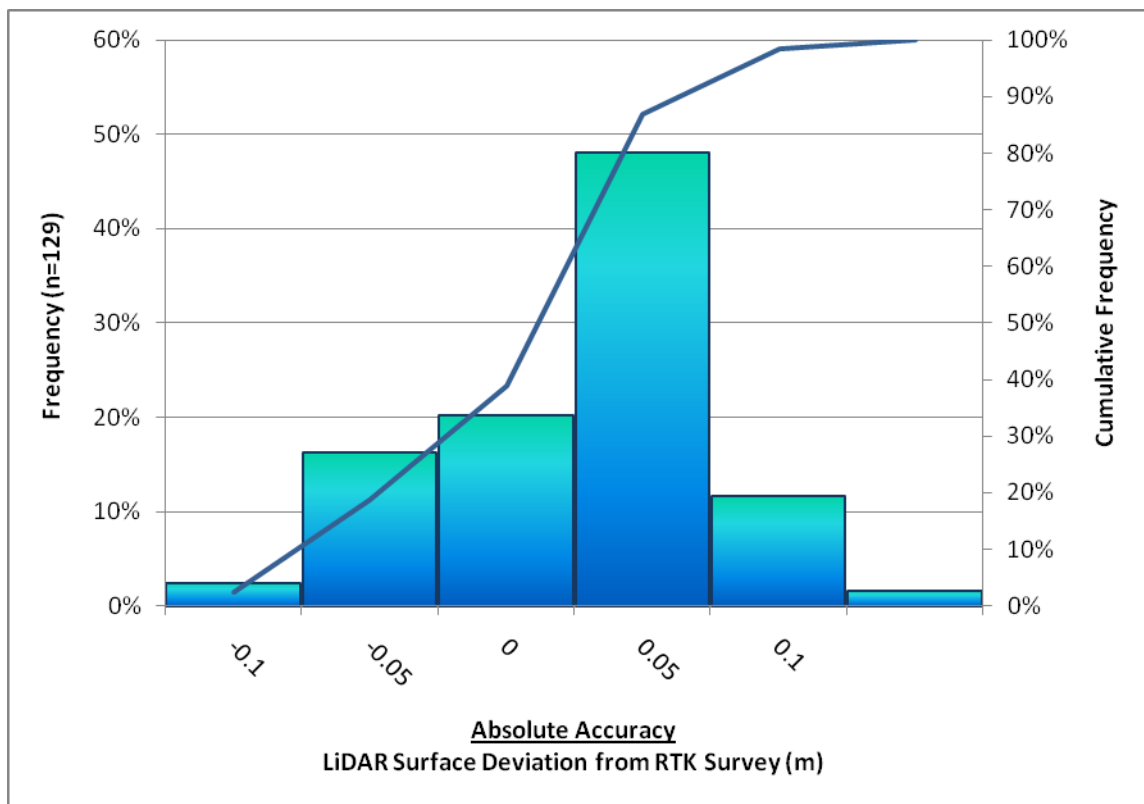
5.4 Absolute Accuracy

Absolute accuracies for the intertidal land within Diablo Canyon Study Area:

Table 4. Absolute Accuracy - Deviation between laser points and RTK survey points.

RTK Survey Sample Size (n): 129		
Root Mean Square Error (RMSE) = 0.05 m		Minimum Δz = -0.12m
Standard Deviations 1 sigma (σ) = 0.04 m 2 sigma (σ): 0.10 m		Maximum Δz = 0.11 m
		Average Δz = 0.00 m

Figure 9. Absolute Accuracy - Histogram Statistics, based on check points collected on hard, bare earth surfaces.

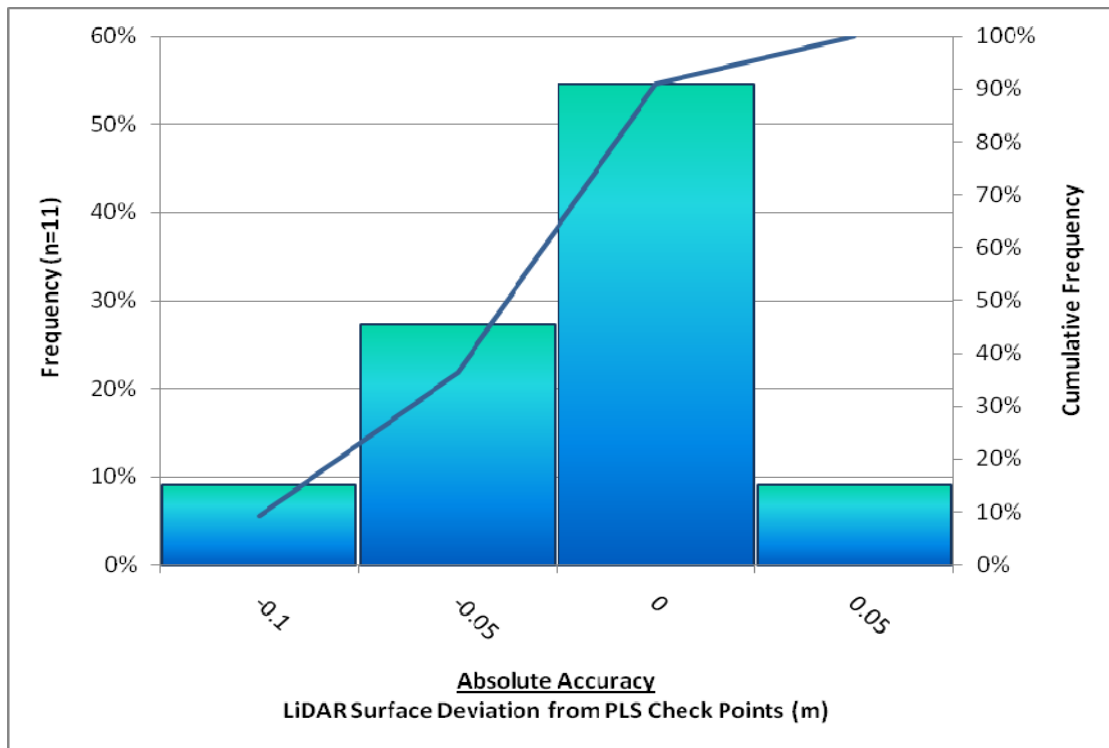


Coordinates were also provided by a professional land surveyor, Mark Sanchez, for 11 points throughout the survey area (Figure 3). The control points were used as an additional test of the absolute accuracy of the LiDAR. Points are tested by comparing their known coordinate elevation with an elevation derived from the LiDAR. The elevation value for the LiDAR is interpolated from the nearest TIN triangle of ground classified points.

Table 5. Absolute Accuracy - Deviation between laser points and PLS Control Check points.

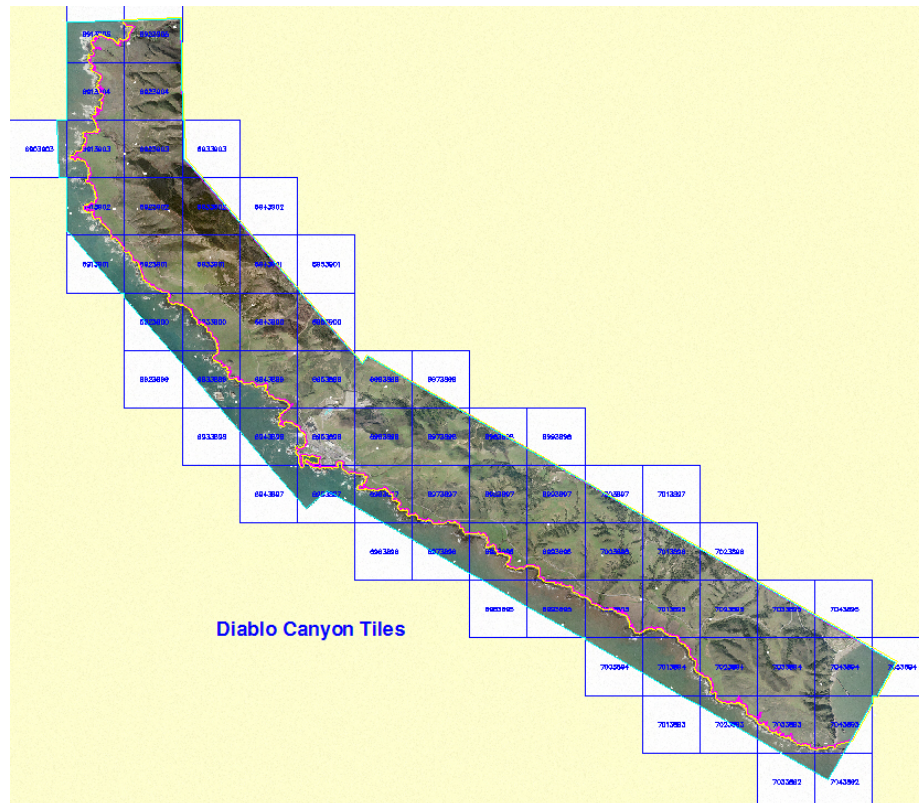
PLS Control Check Points Sample Size (n): 11	
Root Mean Square Error (RMSE) = 0.04 m	Minimum Δz = -0.09 m
Standard Deviations 1 sigma (σ) = 0.05 m 2 sigma (σ): 0.07 m	Maximum Δz = 0.05 m
	Average Δz = 0.01 m

Figure 10. Absolute Accuracy - Histogram Statistics, based on PLS control check points.



6. Orthophotos

Color photography was collected on January 28, 2010 by Tetra Tech Geomatic Technologies Group. Acquisition began at 1:16PM PST and was completed at 1:47PM PST. Six lines of photography were acquired, totaling 44 exposures. Three of the lines were flown slightly offshore to afford a good view of the high bluffs characteristic of the coast at Diablo Canyon. During the collection of those lines the tide ranged from -0.8 to -1.0 feet. The orthophotos were delivered in 55 km² tiles with a pixel resolution of 0.2m.



7. WSI Deliverables

Point Data:	All laser returns, ground classified (LAS format)
Vector Data:	Processing tile delineation (shapefile format)
Data Report:	Full Report containing introduction, methodology, and accuracy

8. Selected Images

Figure 11. Looking southeast along Diablo Canyon Road. Images are derived from LIDAR point cloud colored by height and textured by intensity.

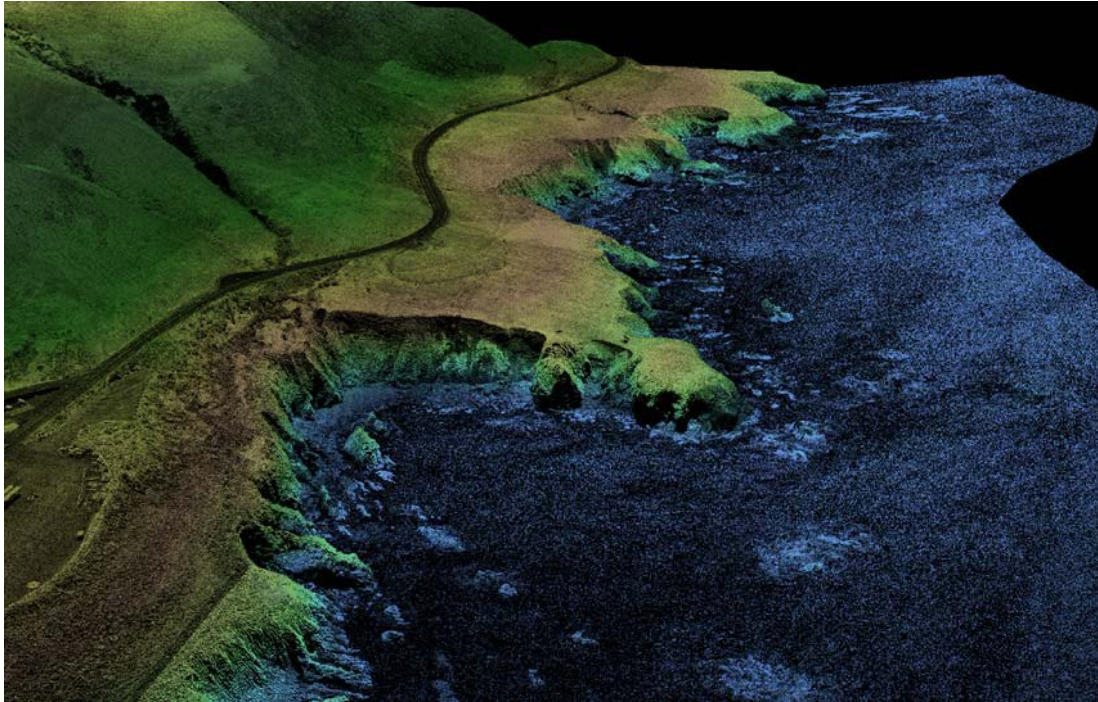


Figure 12. Looking southeast along Diablo Canyon Road. Images are derived from LIDAR point cloud colored by height and textured by intensity.

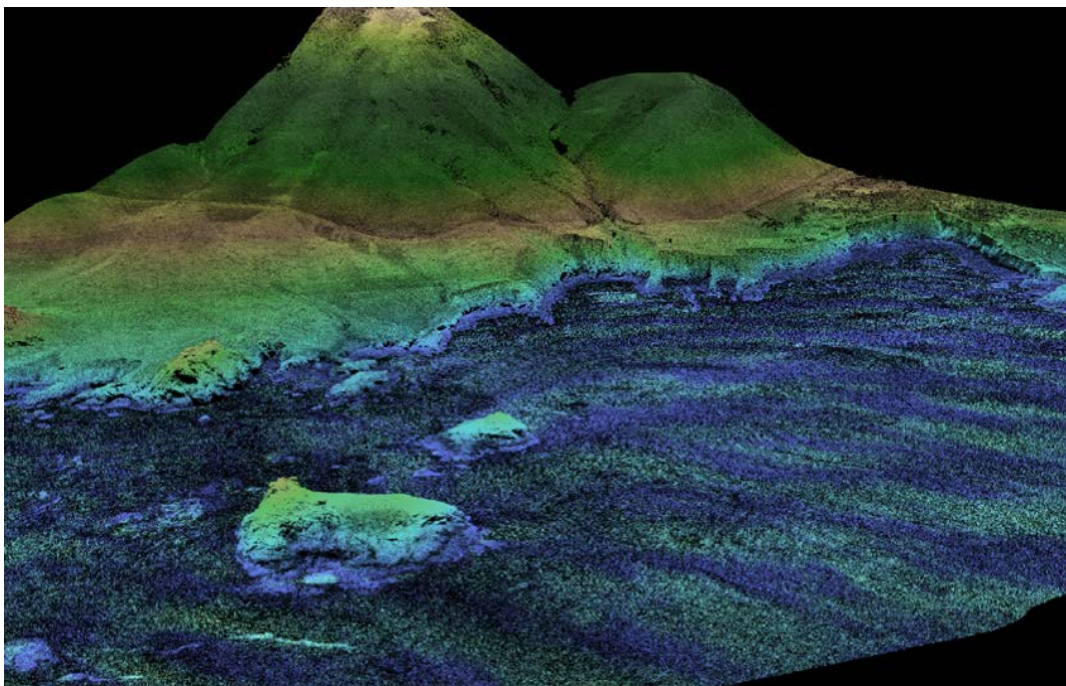


Figure 13. Looking southeast along Diablo Canyon Road at Diablo Canyon Nuclear Generating Station. Images are derived from LIDAR point cloud colored by height and textured by intensity.

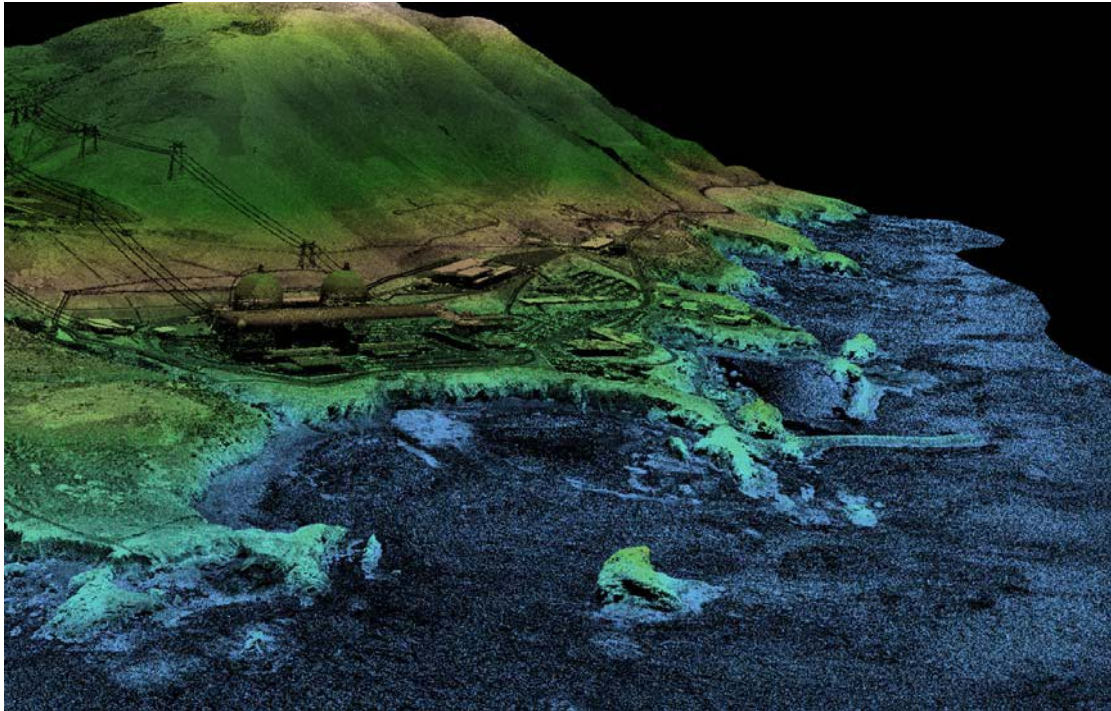


Figure 14. Looking east southeast at Islay Creek meeting the Pacific Ocean in the northern section of the study area. Images are derived from LIDAR point cloud colored by height and textured by intensity.

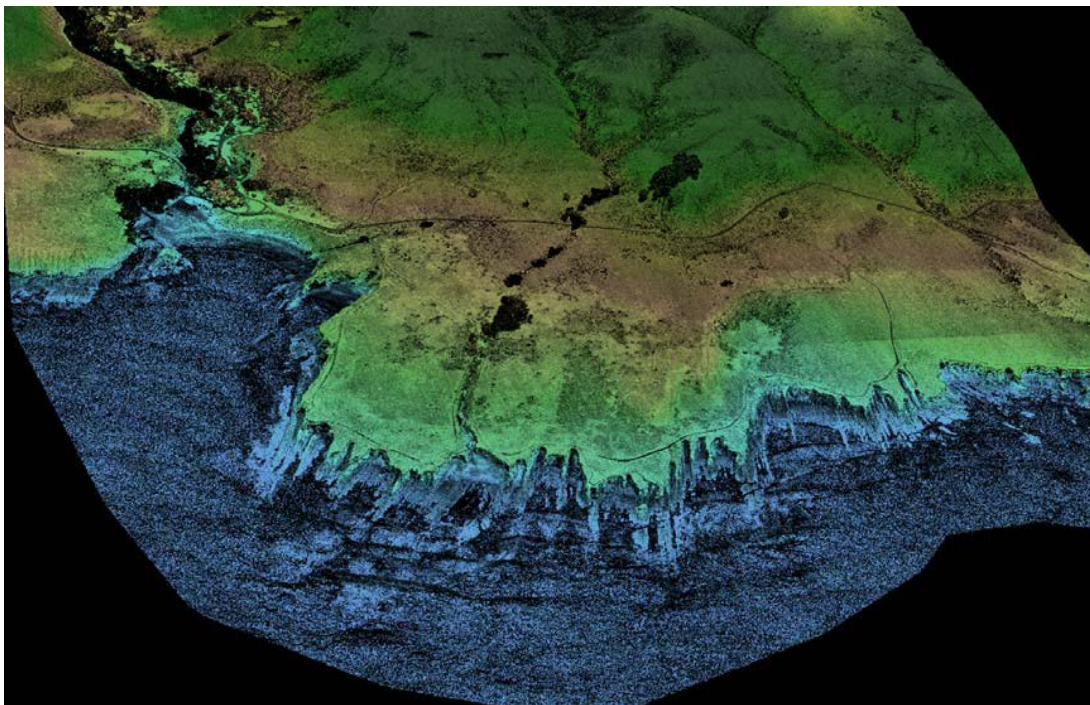


Figure 15. Looking south along coastline of the northern section of the study area. Ortho Imagery draped over highest hit model.



Figure 16. Looking north along coastline of the northern section of the study area. Ortho Imagery draped over highest hit model.



9. Glossary

1-sigma (σ) Absolute Deviation: Value for which the data are within one standard deviation (approximately 68th percentile) of a normally distributed data set.

2-sigma (σ) Absolute Deviation: Value for which the data are within two standard deviations (approximately 95th percentile) of a normally distributed data set.

Root Mean Square Error (RMSE): A statistic used to approximate the difference between real-world points and the LiDAR points. It is calculated by squaring all the values, then taking the average of the squares and taking the square root of the average.

Pulse Rate (PR): The rate at which laser pulses are emitted from the sensor; typically measured as thousands of pulses per second (kHz).

Pulse Returns: For every laser pulse emitted, the Leica ALS 50 Phase II system can record *up to four* wave forms reflected back to the sensor. Portions of the wave form that return earliest are the highest element in multi-tiered surfaces such as vegetation. Portions of the wave form that return last are the lowest element in multi-tiered surfaces.

Accuracy: The statistical comparison between known (surveyed) points and laser points. Typically measured as the standard deviation (sigma, σ) and root mean square error (RMSE).

Intensity Values: The peak power ratio of the laser return to the emitted laser. It is a function of surface reflectivity.

Data Density: A common measure of LiDAR resolution, measured as points per square meter.

Spot Spacing: Also a measure of LiDAR resolution, measured as the average distance between laser points.

Nadir: A single point or locus of points on the surface of the earth directly below a sensor as it progresses along its flight line.

Scan Angle: The angle from nadir to the edge of the scan, measured in degrees. Laser point accuracy typically decreases as scan angles increase.

Overlap: The area shared between flight lines, typically measured in percents; 100% overlap is essential to ensure complete coverage and reduce laser shadows.

DTM / DEM: These often-interchanged terms refer to models made from laser points. The digital elevation model (DEM) refers to all surfaces, including bare ground and vegetation, while the digital terrain model (DTM) refers only to those points classified as ground.

Real-Time Kinematic (RTK) Survey: GPS surveying is conducted with a GPS base station deployed over a known monument with a radio connection to a GPS rover. Both the base station and rover receive differential GPS data and the baseline correction is solved between the two. This type of ground survey is accurate to 1.5 cm or less.

10. Citations

Soininen, A. 2004. TerraScan User's Guide. TerraSolid.

Appendix A

LiDAR accuracy error sources and solutions:

Type of Error	Source	Post Processing Solution
GPS (Static/Kinematic)	Long Base Lines	None
	Poor Satellite	None
	Poor Antenna Visibility	Reduce Visibility Mask
Relative Accuracy	Poor System Calibration	Recalibrate IMU and sensor offsets/settings
	Inaccurate System	None
Laser Noise	Poor Laser Timing	None
	Poor Laser Reception	None
	Poor Laser Power	None
	Irregular Laser Shape	None

Operational measures taken to improve relative accuracy:

1. Low Flight Altitude: Terrain following is employed to maintain a constant above ground level (AGL). Laser horizontal errors are a function of flight altitude above ground (i.e., ~ 1/3000th AGL flight altitude).
2. Focus Laser Power at narrow beam footprint: A laser return must be received by the system above a power threshold to accurately record a measurement. The strength of the laser return is a function of laser emission power, laser footprint, flight altitude and the reflectivity of the target. While surface reflectivity cannot be controlled, laser power can be increased and low flight altitudes can be maintained.
3. Reduced Scan Angle: Edge-of-scan data can become inaccurate. The scan angle was reduced to a maximum of 314° from nadir, creating a narrow swath width and greatly reducing laser shadows from trees and buildings.
4. Quality GPS: Flights took place during optimal GPS conditions (e.g., 6 or more satellites and PDOP [Position Dilution of Precision] less than 3.0). Before each flight, the PDOP was determined for the survey day. During all flight times, a dual frequency DGPS base station recording at 1-second epochs was utilized and a maximum baseline length between the aircraft and the control points was less than 19 km (11.5 miles) at all times.
5. Ground Survey: Ground survey point accuracy (i.e. <1.5 cm RMSE) occurs during optimal PDOP ranges and targets a minimal baseline distance of 4 miles between GPS rover and base. Robust statistics are, in part, a function of sample size (n) and distribution. Ground survey RTK points are distributed to the extent possible throughout multiple flight lines and across the study area.
6. 50% Side-Lap (100% Overlap): Overlapping areas are optimized for relative accuracy testing. Laser shadowing is minimized to help increase target acquisition from multiple scan angles. Ideally, with a 50% side-lap, the most nadir portion of one flight line coincides with the edge (least nadir) portion of overlapping flight lines. A minimum of 50% side-lap with terrain-followed acquisition prevents data gaps.
7. Opposing Flight Lines: All overlapping flight lines are opposing. Pitch, roll and heading errors are amplified by a factor of two relative to the adjacent flight line(s), making misalignments easier to detect and resolve.